



A small diameter, fibrous vascular conduit generated from a poly(ester urethane)urea and phospholipid polymer blend

Yi Hong^{a,b,c}, Sang-Ho Ye^{a,c}, Alejandro Nieponice^{a,b,c}, Lorenzo Soletti^{a,b,d}, David A. Vorp^{a,b,c,d}, William R. Wagner^{a,b,c,d,e,*}

^a McGowan Institute for Regenerative Medicine, University of Pittsburgh, Pittsburgh, PA 15219, USA

^b Center for Vascular Remodeling and Regeneration, University of Pittsburgh, Pittsburgh, PA 15219, USA

^c Department of Surgery, University of Pittsburgh, Pittsburgh, PA 15219, USA

^d Department of Bioengineering, University of Pittsburgh, Pittsburgh, PA 15219, USA

^e Department of Chemical Engineering, University of Pittsburgh, Pittsburgh, PA 15219, USA

ARTICLE INFO

Article history:

Received 3 December 2008

Accepted 7 January 2009

Available online 1 February 2009

Keywords:

Polyurethane

Phospholipid copolymer

Electrospinning

Small diameter blood vessel

Scaffold

ABSTRACT

The thrombotic and hyperplastic limitations associated with synthetic small diameter vascular grafts have generated sustained interest in finding a tissue engineering solution for autologous vascular segment generation *in situ*. One approach is to place a biodegradable scaffold at the site that would provide acute mechanical support while vascular tissue develops. To generate a scaffold that possessed both non-thrombogenic character and mechanical properties appropriate for vascular tissue, a biodegradable poly(ester urethane)urea (PEUU) and non-thrombogenic bioinspired phospholipid polymer, poly(2-methacryloyloxyethyl phosphorylcholine-co-methacryloyloxyethyl butylurethane) (PMBU) were blended at PMBU weight fractions of 0–15% and electrospun to create fibrous scaffolds. The composite scaffolds were flexible with breaking strains exceeding 300%, tensile strengths of 7–10 MPa and compliances of $2.9\text{--}4.4 \times 10^{-4} \text{ mmHg}^{-1}$. *In vitro* platelet deposition on the scaffold surfaces significantly decreased with increasing PMBU content. Rat smooth muscle cell proliferation was also inhibited on PEUU/PMBU blended scaffolds with greater inhibition at higher PMBU content. Fibrous vascular conduits (1.3 mm inner diameter) implanted in the rat abdominal aorta for 8 weeks showed greater patency for grafts with 15% PMBU blending versus PEUU without PMBU (67% versus 40%). A thin neo-intimal layer with endothelial coverage and good anastomotic tissue integration was seen for the PEUU/PMBU vascular grafts. These results are encouraging for further evaluation of this technique in larger diameter applications for longer implant periods.

© 2009 Elsevier Ltd. All rights reserved.

1. Introduction

Autologous vascular segments, primarily the saphenous vein, are routinely used for arterial bypass procedures to address vascular occlusion in coronary and peripheral artery diseases. While venous segments are not ideal, and are susceptible to intimal hyperplasia and accelerated atherosclerosis, they perform much better than synthetic vascular grafts in small diameter applications. Below approximately 4 mm internal diameter, synthetic grafts are rarely employed due to acute failure from thrombotic occlusion or failure in months due to intimal hyperplasia. A tissue engineering

approach which would allow for the ultimate generation of an autologous vascular segment is thus attractive [1]. Using a biodegradable scaffold that would provide acute mechanical support while vascular tissue develops at the site is one approach.

Several vascular scaffolds have been developed based on a variety of hydrolytically labile polyesters [2]. Many of these scaffolding materials are inherently stiff and lack the ability to match the compliance of the native vessels to which a scaffold would be anastomosed. This mechanical mismatch is hypothesized to drive graft failure mechanisms [3]. Thrombus formation occurring soon after blood perfusion would also be a major concern that would limit application of many of these materials as scaffolds for blood vessels developing *in situ*.

Numerous studies have independently evaluated the challenges of developing mechanically appropriate vascular conduits and non-thrombogenic blood contacting surfaces. Compliance matching has been pursued in terms of polymer selection, most notably in the

* Corresponding author. McGowan Institute for Regenerative Medicine, University of Pittsburgh, Pittsburgh, PA 15219, USA. Tel.: +1 412 235 5138; fax: +1 412 235 5110.

E-mail address: wagnerwr@upmc.edu (W.R. Wagner).

development of biodegradable elastomers [4–6], and also in terms of polymer processing [6–8]. To reduce thrombogenicity, some notable techniques including surface or compositional modification with non-thrombogenic substances [9–12], endothelialization [13–15], nitric oxide release [16] and stem cell seeding [17,18] have been developed. The bioinspired phospholipid polymer, 2-methacryloyloxyethyl phosphorylcholine (MPC), and copolymers containing MPC have been utilized to abrogate thrombogenesis on a variety of biomaterials by surface chemical grafting [19,20] and blending [21,22].

Our objective in this study was to develop a compliant conduit that could serve as temporary vascular scaffold and facilitate tissue integration in situ while avoiding acute thrombosis. An electrospun biodegradable elastomer, poly(ester urethane)urea (PEUU, Fig. 1A) was employed as a scaffolding material that would be able to match native vessel compliance while also providing good surgical handling properties. We hypothesized that PEUU alone would not be adequately non-thrombogenic and that a second component would be needed to impart this activity. We thus investigated the processing of blends between PEUU and the MPC-containing copolymer poly(2-methacryloyloxyethyl phosphorylcholine-co-methacryloyloxyethyl butylurethane) (PMBU, Fig. 1B). After evaluating the morphological, mechanical and cell interaction properties of the blended materials in vitro, we electrospun fibrous conduits of 1.3 mm internal diameter for evaluation in vivo as end-to-end aortic replacements in a rat model with an evaluation period of 8 weeks.

2. Materials and methods

2.1. Materials

Polycaprolactone diol (number average molecular weight = 2000, Sigma) was dried under vacuum for 48 h to remove residual water. 1,4-Diisocyanatobutane (Sigma) and putrescine (Sigma) were distilled under vacuum. Dimethyl sulfoxide (DMSO, Sigma) and 1,1,1,3,3,3-hexafluoro-2-propanol (HFIP, Oakwood Products, United States) were used as received. Stannous octoate (Sigma) was dried over 4-Å molecular sieves. PEUU was synthesized as previously reported [23]. Poly(methacryloyloxyethyl phosphorylcholine-co-methacryloyloxyethyl butylurethane) (PMBU) (molar ratio = 30/70), which was synthesized as previously reported [24,25], was kindly provided by Professor Kazuhiko Ishihara of the University of Tokyo, Department of Materials Engineering.

3. Electrospinning of MPC copolymer and PEUU

PEUU in HFIP was blended with PMBU at 0, 5, 10 and 15 wt% (of PEUU) to obtain a 6 wt% solution. The mixed solution was fed at

1 mL/h by syringe pump (Harvard Apparatus, United States) into a steel capillary (inner diameter = 1.2 mm) that was suspended 15 cm over a stainless steel mandrel (19 mm diameter for sheet and 1.3 mm diameter for tube) rotating at 250 rpm. The mandrel was located on an x-y stage (Velmex, United States) that reciprocally translated in the direction of the mandrel axis at a speed of 5 cm/s and with an amplitude of 8 cm. Two high-voltage generators (Gamma High Voltage Research, United States) were employed to charge the steel capillary to 10 kV and the mandrel to -10 kV respectively. Electrospinning of the polymer solution proceeded for approximately 4 h for a sheet or 45 min for a conduit, after which the deposited fibrous sheet or conduit was removed from the big or small mandrel, respectively. The sheets and conduits were dried in a vacuum oven at room temperature overnight. PEUU, PMBU5, PMBU10 and PMBU15 refer to fibrous sheets or conduits constructed from PEUU blended with 0, 5, 10, and 15 wt% PMBU respectively.

3.1. Electrospun sheet and conduit characterization

The morphologies of electrospun PEUU/PMBU blended sheets were observed under scanning electronic microscopy (SEM, JSM-6330F, JEOL) after gold coating. The change of fiber diameter before and after immersion in PBS at 37 °C for 24 h was measured by image processing software ImageJ (NIH, United States).

The surface composition of the samples was analyzed by X-ray photoelectron spectroscopy (XPS) using a Surface Science Instruments S-probe spectrometer with a take-off angle of 55°. This take-off angle corresponds to a sampling depth of approximately 5 nm. Elemental composition spectra were acquired using a pass energy of 150 eV. High-resolution C1s spectra were acquired at an analyzer pass energy of 50 eV. The Service Physics ESCAVB Graphics Viewer program was used to determine peak area, calculate the elemental compositions from peak areas and peak fit the high-resolution spectra. The surface composition on a given sample was averaged from two composition spots and one high-resolution C1s analysis. The mean value for three different samples was determined.

Strips of 2 × 20 × 0.2 mm cut from the electrospun sheet were used for tensile mechanical testing on an MTS Tytron 250 Micro-Force Testing Workstation at a 10 mm/min crosshead speed, according to ASTM D638-98. At least four samples were tested for each sheet.

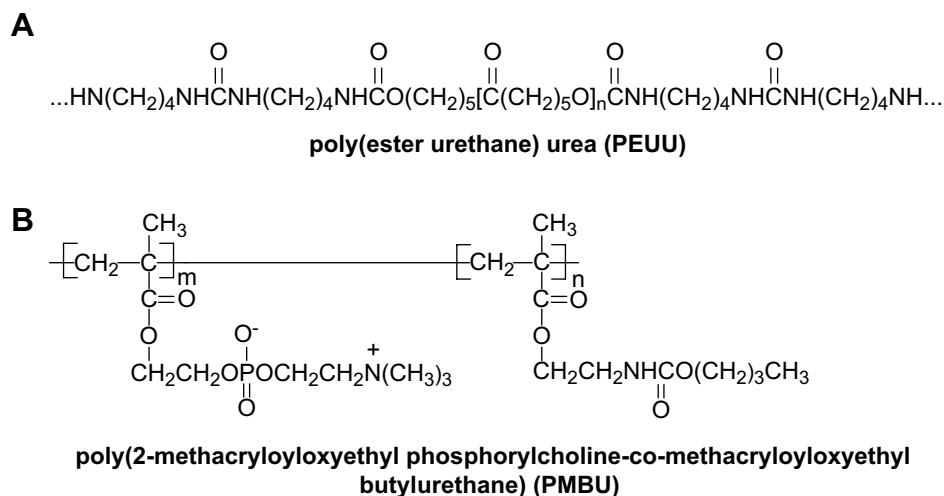


Fig. 1. Chemical structures of (A) PEUU and (B) PMBU.

Dynamic compliance measurements were performed using a previously described perfusion bioreactor system [26]. The system was primed with saline and delivered physiologic, arterial, pulsatile intraluminal pressure (120/80 mmHg) at minimal flow (~ 10 mL/min). Briefly, a Biomedicus centrifugal pump connected via Tygon[®] tubing to a tissue testing chamber produced sinusoidal pulsatile pressure and flow consistent with physiologic values. An additional flow loop consisting of a roller pump (Masterflex, Cole-Parmer, Vernon Hills, IL) and a heat exchanger placed into a water bath (Fisher Scientific) recirculated warm saline into the chamber to maintain a temperature of 37 °C during testing. Two pressure transducers (Model TJE, Honeywell – Sensotec Co., Columbus, OH) placed equidistant upstream and downstream of the vessel centre were used to measure intraluminal pressure. The pressure in the center of the vessel was then calculated as the average between the proximal and distal pressure transducer measurements. The outer diameter of the pressurized scaffolds was measured with a He–Ne laser micrometer (Beta LaserMike, Dayton, OH). Both pressure and diameter signals were automatically recorded at 30 Hz for 1 min. Dynamic compliance, C , was calculated from recordings of pressure, P and outer diameter, OD as:

$$C = \frac{(OD_{120} - OD_{80})}{OD_{80}} \frac{1}{(P_{120} - P_{80})} \quad (1)$$

3.2. Ovine blood platelet deposition

Whole blood was collected with an 18 gauge needle by venipuncture from a healthy ovine donor following NIH guidelines for the care and use of laboratory animals. After discarding the first 3 mL, the collected blood was immediately added to monovette tubes containing 0.3 mL of 0.106 M trisodium citrate (Sarstedt, Newton, NC). Sample disks (7 mm diameter) were incubated in BD Vacutainer[®] tubes containing 5 mL citrated ovine blood and incubated for 4 h at 37 °C under gentle rocking. The samples were then rinsed thoroughly with 50 mL phosphate buffered saline (PBS; BD Biosciences, San Jose, CA) and immersed in 0.5 mL of 2% Triton X-100 solution (Sigma) for 20 min to lyse surface adherent platelets. The number of platelets deposited on the samples was then determined indirectly by a lactate dehydrogenase (LDH) assay with an LDH Cytotoxicity Detection Kit (Takara Bio, Japan) [27]. Calibration of spectrophotometer absorbance results to platelet numbers was accomplished using a calibration curve generated from known dilutions of ovine platelet rich plasma in the lysing solution. To observe the morphology of deposited platelets, samples were incubated with ovine blood as described above. The surfaces were then rinsed with PBS and immersed in a 2.5% glutaraldehyde solution for 2 h at 4 °C. The sample surfaces were observed by SEM after dehydration and sputter coating.

3.3. Rat smooth muscle cell (RSMC) adhesion and growth

Electrospun samples (6 mm diameter) were obtained by standard biopsy punch and sterilized by exposure to the ultraviolet light source in a laminar flow cell culture hood (Class II A/B3 Biological Safety Cabinet). After rinsing thoroughly with PBS, they were fit into the bottom of a 96-well tissue culture plate.

To evaluate RSMC adhesion, 15×10^4 /mL RSMCs were seeded onto the surfaces and after 24 h, mitochondrial activity (MTT assay, Sigma) was evaluated. The attachment ratio was calculated as $OD_{\text{sample}}/OD_{\text{TCPS}} \times 100\%$ (OD : optical density). For cellular proliferation, RSMCs were seeded at density of 5×10^4 /mL. The culture medium (DMEM (Lonza) supplemented with 10% fetal bovine serum (Lonza) and 5% penicillin/streptomycin solution (Lonza)) was

replaced every 2 d. A mitochondrial activity assay was evaluated at 1, 3 and 5 d with tissue culture polystyrene (TCPS) surface as a control.

To qualitatively verify that the mitochondrial assay results corresponded to cell numbers and to evaluate cell morphology, samples at days 1, 3 and 5 were fixed in a 2.5% glutaraldehyde/PBS solution. After PBS rinsing, samples were then immersed in 0.5% Triton X-100 (Sigma) solution for 45 min, and rhodamine phalloidin (1:250, Invitrogen) was added to stain alpha-smooth muscle actin (α -SMA) for 30 min. After washing with PBS three times, cellular nuclei were stained by DRAQ5 (1:1000, Biostatus) for 1 h. After another three PBS rinses, the sample surfaces and cellular morphology were observed under confocal laser scanning microscopy (Olympus Fluoview 500).

3.4. In vivo assessment

A rat model was utilized to compare PEUU and PMBU15 conduits (1.3 mm inner diameter) as segmental aortic replacements following NIH guidelines for the care and use of laboratory animals. Young Lewis rats (female, 300 g, Charles River Laboratories) were anesthetized with isoflurane (2% for the induction and 1% for the maintenance) and a single dose of 5 mg/100 g ketamine IM. Briefly, a midline laparotomy incision was made and the abdominal aorta exposed below the renal arteries. Microclamps were applied to the infrarenal aorta, proximally and distally, and the vessel was sectioned in between the clamps creating a gap of approximately 1 cm. The PEUU (control) and PMBU15 grafts to be implanted were trimmed on both edges to obtain a 1 cm long construct and then sutured in place to the native aorta in an end-to-end interrupted anastomotic pattern with 10.0 prolene (Johnson & Johnson). Finally, the muscle layer and skin were closed with 3-0 polyglactin absorbable suture (VICRYL, Ethicon, Inc.). Anti-platelet therapy was started after the surgery with aspirin and dipyridamole (200 mg PO daily during the first week and 100 mg PO daily after the first week until elective sacrifice). After 8 weeks, rats were heparinized, sacrificed and fluoroscopy was immediately performed to evaluate vessel patency. The aorta was explanted with native tissue segments above and below the vascular graft, and this tissue was fixed in a 10% formaldehyde solution. Images of the longitudinal section were observed under SEM (Hitachi S-2460N) after dehydration and gold coating. Masson trichrome staining was performed on paraffin embedded sections, while immunohistologic staining utilized cryosections. α -SMA was stained by a mouse monoclonal antibody to α -SMA (Chemicon), followed by CY3 goat anti-mouse antibody (Jackson). Von Willebrand factor (vWF) was stained using a rabbit anti-human antibody to vWF (DAKO), followed by alexa fluor 488 goat anti-rabbit IgG (H + L) (Invitrogen). The fluorescent images were observed under a fluorescent microscopy (Nikon E-600).

3.5. Statistical analysis

Results are displayed as the mean \pm standard deviation. One-way ANOVA was utilized to evaluate the fiber diameter, mechanical properties and biological results using the Neuman–Keuls test for post-hoc assessment of the differences between specific samples. Significance was considered to exist at $p < 0.05$.

4. Results

4.1. Electrospun sheet and conduit characterization

As shown in Fig. 2, a uniform PEUU/PMBU blend fibrous tube with an inner diameter of 1.3 mm, length of approximately 5 cm and wall thickness of approximately 300 μm was fabricated by

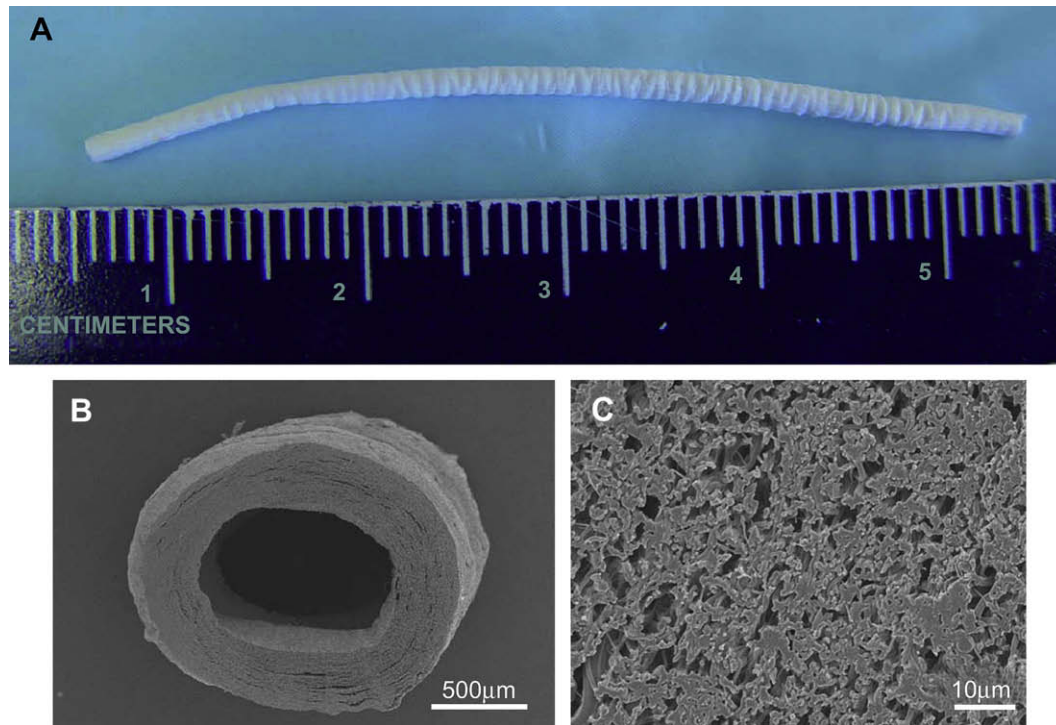


Fig. 2. (A) Macrographic image of typical small diameter electrospun PEUU/PMBU blend tube (PMBU15). (B) Cross-sectional SEM image of the vascular conduit at low and (C) high magnifications.

electrospinning. The fibrous morphology of scaffolds generated from different PMBU contents (Fig. 3) exhibited continuous, smooth sub-micron fibers without beading at all PMBU mass fractions (0, 5, 10, 15%). No obvious trend was found in morphology with PMBU content change. The fiber diameters at different PMBU contents showed no significant differences and were approximately 500 nm (Table 1). The stability of the fibers in an aqueous environment was reflected in the fiber diameters measured after 24 h immersion in PBS at 37 °C, where no significant change in fiber diameters was observed (Table 1). High-resolution ESCA analysis of the electrospun surfaces revealed an extra N1s peak at 402.5 eV ($-\text{N}(\text{CH}_3)_3$), which was attributed to PMBU in the blend scaffolds. PEUU scaffolds were found to have only one N1s peak at 399.5 eV (amide bond) (data not shown). At the same time, the surface N/C and P/C ratios increased from 2.6 to 5.8% and from 0 to 1.23% respectively with increase of PMBU content in the scaffolds (Table 2).

The mechanical properties of the fibrous sheets and conduits are summarized in Table 3. Pure PEUU fibrous sheet has tensile strength of 9 ± 1 MPa and breaking strain of $388 \pm 58\%$. With PMBU addition, there was minimal effect on the tensile strength, breaking strain, initial modulus or 100% modulus with all parameters being statistically equivalent to pure PEUU with the exception of a slight decrease in tensile strength for PMBU15 ($p < 0.05$). Evaluation of conduit compliance in 1.3 mm inner diameter tubes similarly demonstrated no significant differences between PEUU/PMBU blends and pure PEUU. Compliance values ranged from $2.9 \pm 0.6 \times 10^{-4}$ to $4.4 \pm 1.1 \times 10^{-4}$ mmHg $^{-1}$.

4.2. *In vitro* ovine platelet deposition

Following whole blood incubation to evaluate surface thrombogenicity, electron micrographs of the electrospun surfaces (Fig. 4) qualitatively demonstrated a marked decrease in platelet

deposition with increasing PMBU content. After 4 h of blood contact a large number of platelet aggregates were apparent on PEUU surfaces with some pseudopodia extensions (Fig. 4A and D). For PMBU5 aggregates were sparse and comprised of only a few platelets, although individual adherent platelets were plentiful. Pseudopodia extension was present, but at low levels and not accompanied by substantial platelet spreading (Fig. 4B and E) At a PMBU content of 10%, only sparse single platelets were found to be adherent on the surface with no apparent pseudopodia (Fig. 4C and F). Finally, at 15% PMBU (Fig. 4D and G), the surfaces were largely devoid of platelet adhesion.

Platelet deposition was quantified with the LDH assay as shown in Fig. 5. All PMBU blend sheets experienced significantly lower deposition than the PEUU sheet ($p < 0.05$). The deposited platelet number on the surfaces of PMBU10 and PMBU15 was similar ($p > 0.05$), but much lower than that of PMBU5 ($p < 0.05$).

4.3. *In vitro* RSMC adhesion and growth

Smooth muscle cell adhesion (as reflected in mitochondrial activity) at 24 h from a relatively high seeding density onto PEUU and PEUU/PMBU blend surfaces is reported in Fig. 6A in terms of relative cell number compared to TCPS (a positive control surface representing 100% adhesion value here). A statistically equivalent number of RSMCs attached to the PEUU surface and the TCPS control. Both PEUU and TCPS had significantly higher cell adhesion indices, than PMBU blended sheets, which had 70–76% of TCPS values. There were no significant differences between the three PMBU content sheets. In Fig. 6B RSMC proliferation, (again reflected in terms of mitochondrial activity relative to TCPS at day 1) is shown for days 1, 3 and 5 on PEUU and PEUU/PMBU blended sheets. RSMC viability increased with time on PEUU, PMBU5 and PMBU10 sheets, although relative cell numbers were lower at day 5 with increasing PMBU content. RSMC viability values at days 3 and 5

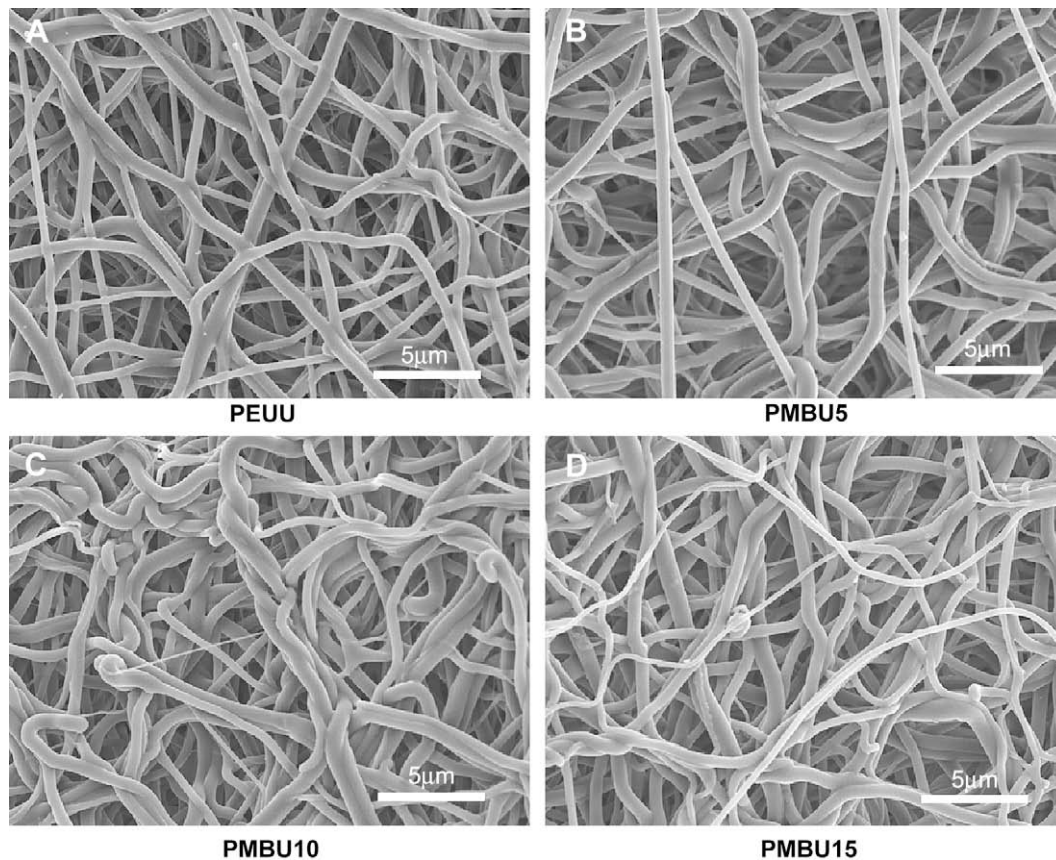


Fig. 3. Fiber morphologies of PEUU and PEUU/PMBU blend sheets at (A) 0%, (B) 5%, (C) 10% and (D) 15% PMBU.

Table 1

Fiber diameter before and after 24 h PBS immersion at 37 °C.

Sample	Before (nm)	After (nm)
PEUU	476 ± 161	469 ± 150
PMBU5	532 ± 145	559 ± 130
PMBU10	496 ± 123	448 ± 65
PMBU15	525 ± 162	519 ± 167

were much higher than that of PMBU15 ($p < 0.05$). Further, during the 5 day culture RSMC viability on PMBU15 increased at day 3, but unlike the other PMBU blends, then significantly decreased at day 5 ($p < 0.05$).

To verify that the mitochondrial activity data of Fig. 5 were indeed reflective of cell numbers and to investigate cell morphology on PEUU and PEUU/PMBU blend sheets confocal laser scanning microscopy was used to image RSMC f-actin and nuclei in Fig. 7. At day 1, all RSMCs possessed a spread shape on PEUU (Fig. 7A) and PMBU5 (Fig. 7D), although to a qualitatively lesser extent for the latter. A mixture of spread and rounded cells was present on the PMBU10 surface (Fig. 7G) whereas all cells on the

Table 2

Surface atomic composition ratio determined by XPS.

Sample	N/C ratio (%)	P/C ratio (%)
PEUU	2.6 ± 0.4	0
PMBU5	3.5 ± 0.2	0.54 ± 0.01
PMBU10	4.0 ± 0.3	0.73 ± 0.08
PMBU15	5.8 ± 0.3	1.23 ± 0.09

PMBU15 surface (Fig. 7J) were round in shape. At day 3, cell number increased on PEUU (Fig. 7B) and PMBU5 (Fig. 7E), and at day 5, a nearly confluent cell layer had formed on both surfaces (Fig. 7C and F). On the PMBU10 surface, more cells were spread at day 3 (Fig. 7H) and at day 5 almost all cells showed a spread shape and cell number was increased (Fig. 7I). On the PMBU15 surface, no cell spreading was observed at day 3 or 5 and cells remained sparse (Fig. 7K and L).

4.4. In vivo testing

After 8 weeks, PMBU15 grafts had a 67% (6/9) patency rate while the control PEUU grafts were 40% patent (10/25) via fluoroscopy. As shown in Fig. 8, the aorta (deep black line) in the representative fluorography for the PEUU grafted animals was blocked at the implant site (arrow) (Fig. 8A), but the aorta was open to contrast media in the representative fluorography of the PMBU15 grafted rats (Fig. 8B). As shown in Fig. 8C, the lumens of PMBU15 grafts were generally clear and devoid of thrombotic

Table 3

Summary of mechanical properties.^a

Sample	Stress (MPa)	Strain (%)	Initial modulus (MPa)	Modulus at 100% (MPa)	Compliance ($\times 10^{-4}$ mmHg ⁻¹)
PEUU	9 ± 1	388 ± 58	5 ± 3	2 ± 1	2.9 ± 0.6
PMBU5	10 ± 1	324 ± 26	5 ± 2	3 ± 1	3.8 ± 1.8
PMBU10	10 ± 1	301 ± 76	5 ± 1	3 ± 1	3.7 ± 1.0
PMBU15	7 ± 1	342 ± 43	7 ± 3	3 ± 1	4.4 ± 1.1

^a Compliance was determined in 1.3 mm inner diameter conduits, other parameters utilized strips obtained from electrospun sheets in tensile testing.

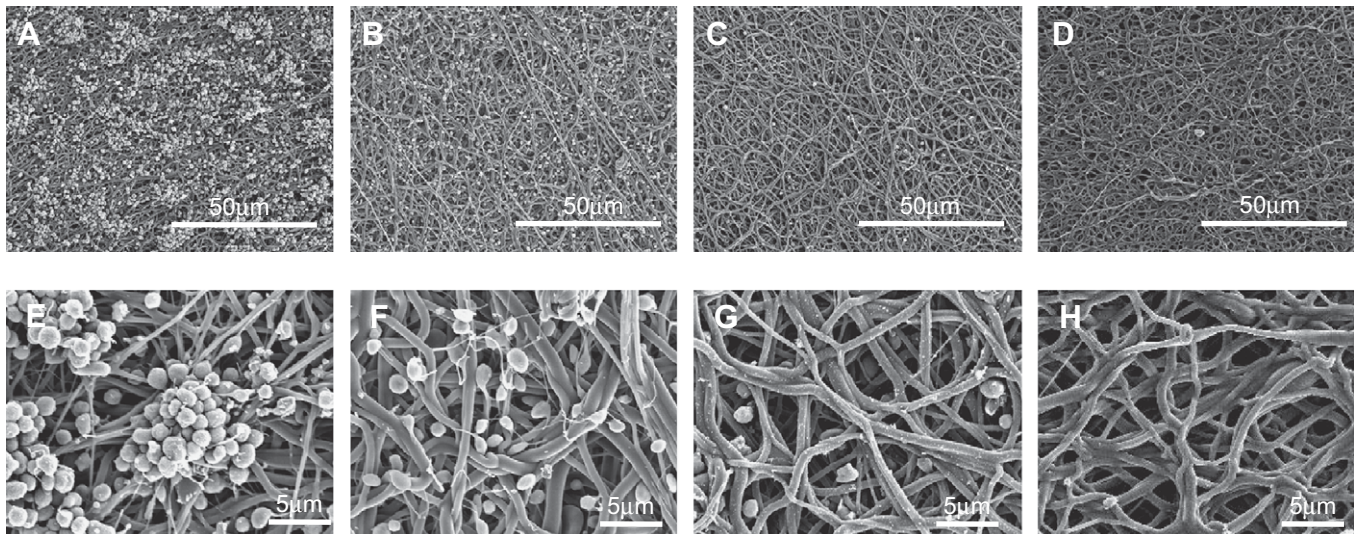


Fig. 4. Electron micrographs of sheets following ovine blood contact (A, E) PEUU, (B, F) PMBU5, (C, G) PMBU10 and (D, H) PMBU15.

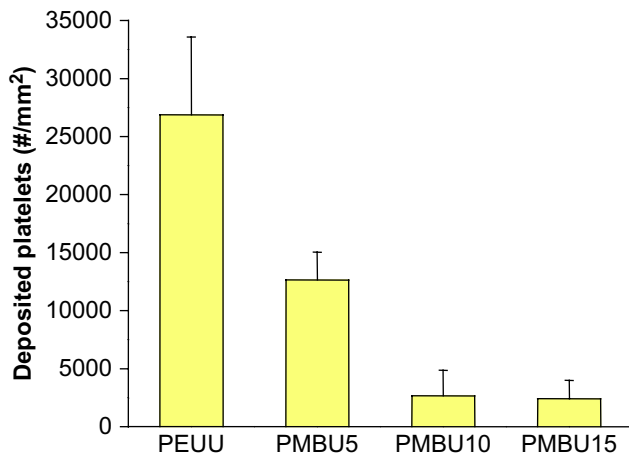


Fig. 5. Ovine blood platelet deposition on electrospun PEUU/PMBU blend sheets after ovine blood contact using the LDH assay.

deposition or obvious intimal hyperplasia. An electron micrograph of a longitudinal section covering the anastomotic region between native aorta and PMBU15 graft shows good continuity with qualitative indications of a continuous endothelium (Fig. 8D). Masson trichrome staining of transverse (Fig. 9A and B) and longitudinal (Fig. 9C and D) sections of PMBU15 grafts showed a continuous cellular layer comprising an intimal layer which exhibited collagen and cellular components. Cell body orientation was in the direction of flow. Minimal cellular infiltration into the graft wall was observed and polymer volume or mass loss was not apparent. For the typical PEUU graft the lumen was filled due to thrombosis (with subsequent organization) or intimal hyperplasia (Fig. 9E). Continuity with the native aortic tissue, shown in Fig. 8D, is seen in longitudinal section of Fig. 9C for both the luminal and advential surfaces.

Further characterization of the cells populating the PMBU15 grafted segment with immunohistochemical staining is shown in Fig. 10. Staining was consistent with a luminal layer comprised of underlying myofibroblasts or smooth muscle cells (positive α -SMA staining) and a blood contacting surface of vWF positive endothelial cells.

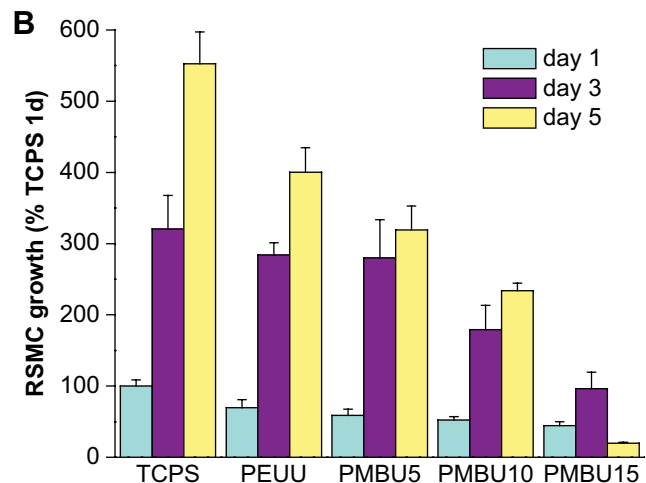
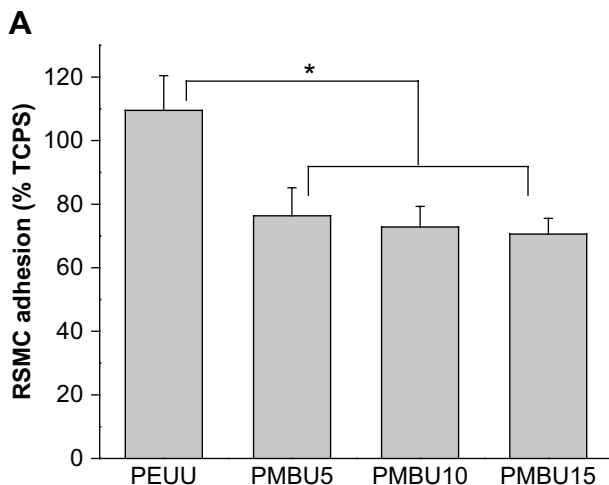


Fig. 6. Relative rat smooth muscle cell (A) adhesion and (B) growth on electrospun PEUU/PMBU blend sheets in terms of mitochondrial activity. Data are normalized to TCPS at 24 h.

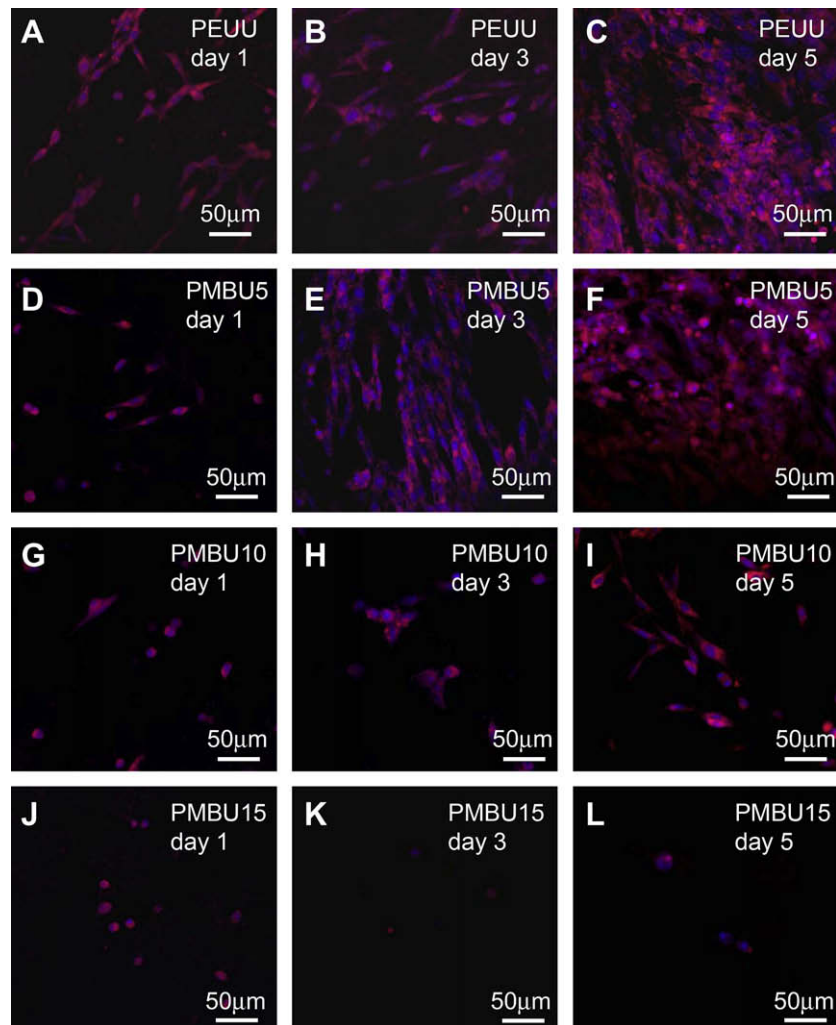


Fig. 7. Confocal images of RSMC morphology after seeding on electrospun PEUU/PMBU blend sheets (PEUU, PMBU5, PMBU10 and PMBU15) at days 1, 3 and 5. F-actin (red) was stained with rhodamine phalloidin and nuclei (blue) were stained with DRAQ5. Scale bar is 50 μm .

5. Discussion

Tissue engineering approaches to the generation of small diameter vascular grafts can be divided into those in which a scaffold is seeded with cells, potentially cultured for some development period *in vitro*, and then implanted, or those approaches where the scaffold is capable of serving as a functional replacement without cell seeding or culture. In the latter case cellular ingrowth is expected to ultimately generate a functional replacement. Scaffolds for vascular graft engineering are required to be biodegradable and possess appropriate mechanical properties for the culture period, or at least at the time of implant. Biocompatibility considerations will vary. A scaffold that is seeded and effectively covered with cells may not need to be non-thrombogenic and the support of cell adhesion may initially be desirable. Non-seeded scaffolds must meet high levels of thromboresistance to avoid acute failure upon initiation of luminal blood flow, but ultimately must allow native tissue to develop as the scaffold degrades. Depending upon the degradation rate of the scaffold, the proliferation of smooth muscle cells should occur, but preferably not in a manner that would lead to lumen compromise due to hyperplasia.

Many approaches have been pursued for acellular biodegradable vascular grafts. Decellularized tissues evaluated include canine jugular vein [28], carotid artery [29] or aorta [30], ovine carotid

artery or aorta [31] and pig carotid artery [32]. These approaches have been pursued in the absence of cross-linking agents to modify the remaining extracellular matrix components. Synthetic scaffold materials have included poly(lactide-co-caprolactone) [14], polylactide [33], polycaprolactone [34], poly(lactide-co-glycolide) [35], polydioxanone [36], poly(diethyl citrate) [5], poly(glycerol sebacate) [4] and polyhydroxyalkanoate [37]. These materials have been generated with numerous techniques including wet-spinning [38], salt leaching [39], thermally induced phase separation [6,35], electrospinning [8,14,15,34,36] and combination approaches [5,33,40–42]. Synthetic polymers have also been blended with structural biomacromolecules collagen and elastin during graft processing [8,15,36,43].

There have been several recent reports presenting *in vivo* data for biodegradable polymer based small diameter vascular grafts. Nottelet et al. reported on the implantation of electrospun poly(caprolactone) 2 mm diameter conduits in the rat abdominal aortic position in a pilot study that showed good cellular ingrowth and patency after a 12 week implantation period [34]. He et al. showed patency in three rabbits with electrospun poly(lactide-co-caprolactone) conduits (1 mm inner diameter) after 7 weeks in a venous placement model, however no endothelial cell layer was found to have formed on the luminal surface [14]. A non-woven composite conduit less than 1 mm in diameter and based on polyglycolic acid/

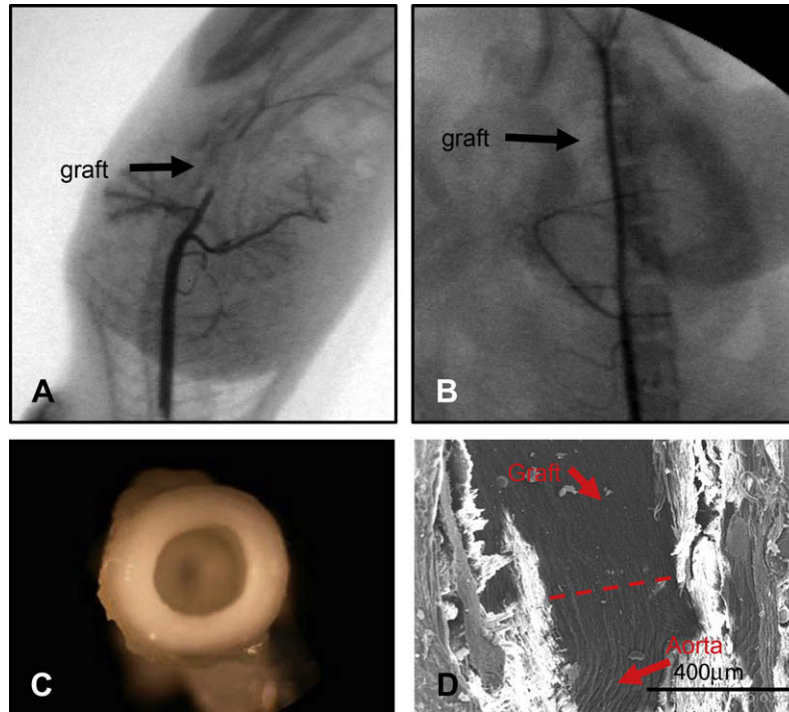


Fig. 8. Fluoroscopic images of (A) PEUU grafted aorta and (B) PMBU15 grafted aorta after 8 week implantation period in the rat model. (C) Macroscopic image of PMBU15 graft at the time of explant. (D) Electron micrograph of a longitudinal section from PMBU15 graft after explant. Dashed line reflects transition from native aorta to graft.

poly(lactide-co-caprolactone) or polylactic acid/poly(lactide-co-caprolactone) possessed excellent patency without thrombogenicity after 3 weeks of implantation in an SCID/bg mouse, and endothelialization and collagen deposition were observed on the

lumen after a 6 week period [40]. Tillman et al. utilized an electrospun blend of poly(caprolactone) and collagen to generate 5 mm inner diameter conduits for implantation in a rabbit aortoiliac bypass model and found a majority of the grafts to be patent after

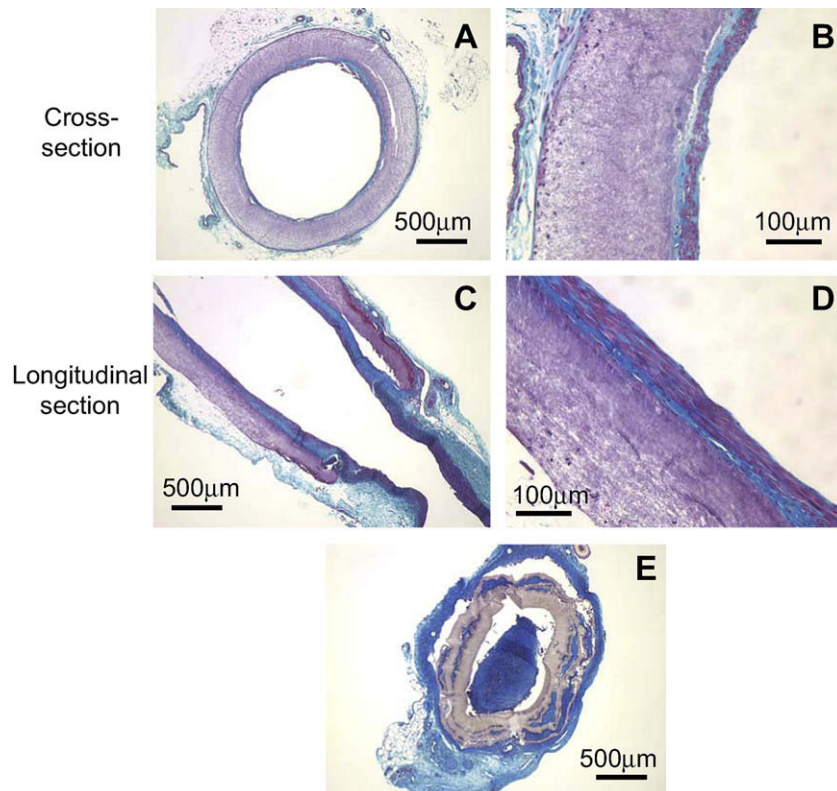


Fig. 9. Masson trichrome staining of PMBU15 and PEUU grafts at the 8 week explant. Images (A) and (B) are transverse cross-sections of a PMBU15 graft, and (C) and (D) are the longitudinal sections of a PMBU15 graft. Image (E) is a transverse cross-section of a PEUU control graft that was occluded.

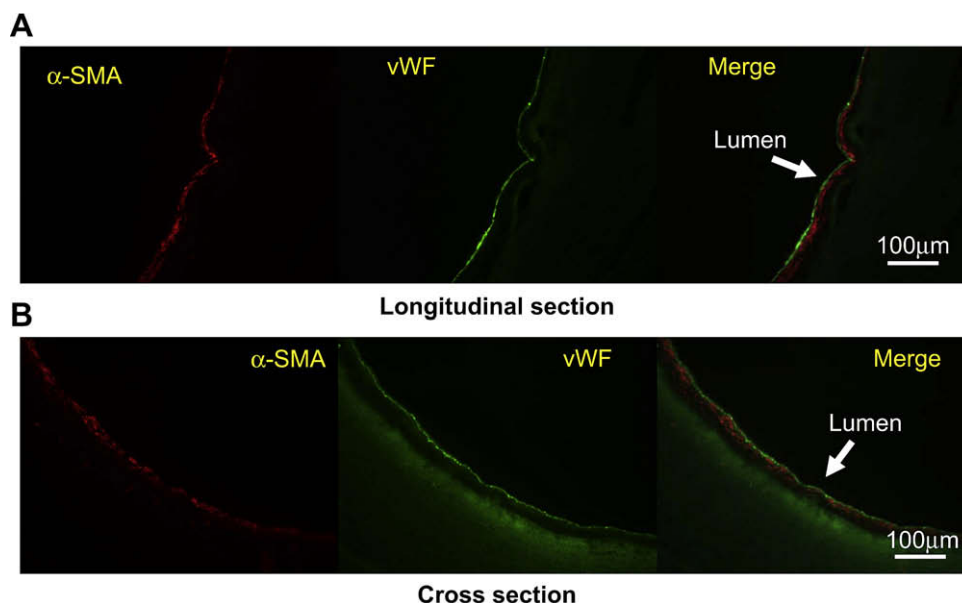


Fig. 10. Immunohistochemical staining of PMBU15 graft after 8 week implantation period. The images in (A) are longitudinal sections stained for α -SMA (red), vWF (green) and a merged image of these two sections. The images in (B) are similarly stained transverse cross-sections. The polymer exhibits some fluorescence at the green wavelength imaged.

a one month implantation period, although platelet deposition was observed on grafts after blood exposure in the initial part of the study [15].

The biodegradable thermoplastic elastomer utilized in this report, PEUU, has been shown to possess attractive mechanical properties for soft tissue applications [23] and an ability to be processed into a porous scaffolds by thermally induced phase separation [6,44], and sub-micron fibrous scaffolds by electrospinning [45]. Previous *in vivo* studies with this polymer have demonstrated a degradation rate that varies with implantation site and processing method [46–48]. For vascular graft applications, approaches in which PEUU is combined with cells are under investigation [15,49] and show promise for future *in vivo* investigation. However, an approach that avoids cell sourcing and integration would have advantages from a cost, lead time and regulatory perspective.

Mechanically, the electrospun PEUU vascular conduits reported here possessed mechanical properties amenable to vascular application with compliance values comparable to a human artery [50]. Surgical handling was qualitatively found to be good, with no bleeding from suture sites and good suture retention strength. One would not inherently assume PEUU to be thromboresistive, although in some settings such as the right ventricular outflow tract in the rat an alternatively processed PEUU did not show evidence of thrombotic complications [46]. In the current report, electrospun PEUU vascular conduits were not found to be adequately non-thrombogenic or resistant to intimal hyperplasia in the rat abdominal aorta model with high rates of vascular occlusion observed. This result is not particularly surprising given that the challenge of resisting thrombosis and hyperplasia in such a small diameter vascular graft is well known to be high and that PEUU was shown here to be supportive of platelet deposition and smooth muscle cell adhesion.

Blending with the PMBU polymer markedly reduced platelet and smooth muscle cell adhesion *in vitro* and these results appeared to directly translate *in vivo* with an increase in graft patency. This effect is most likely due to the presentation of MPC moieties on the polymer blend surface, as evidenced by the ESCA data. Previous reports with MPC-based polymers have shown

reduced cellular affinity that may be related to the high surface free water fraction due to the zwitterionic nature of MPC, resistance to protein adsorption, limited plasma protein activation, and lateral mobility of molecules [51–53]. In addition to being associated with non-thrombogenicity, MPC copolymers have also been shown to suppress inflammatory reactions [54] and to possess negligible cytotoxicity [55]. In the field of small diameter vascular grafts, a seamless 2 mm inner diameter conduit composed of non-degradable segmented polyurethane (SPU, Tecoflex 60) blended with an MPC-containing copolymer was implanted into rabbit carotid arteries for 7 days without fibrin deposit and platelet aggregation [22]. In a subsequent study a polyester prosthesis was coated with a SPU/10% MPC copolymer blend and implanted into rabbit carotid arteries for 8 weeks where it was found to be non-thrombogenic and apparently lacked both smooth muscle and endothelial cells on the lumen [56]. These previous results motivated our exploration of a small diameter vascular conduit based upon a blend of the biodegradable PEUU and a polyurethane compatible MPC-containing copolymer. We hypothesized that the MPC copolymer would acutely inhibit thrombogenesis and hyperplasia, but that with scaffold degradation autologous tissue replacement would occur.

Many previously described MPC-containing copolymers possess high hydrophilicity, and do not blend uniformly with the relatively hydrophobic PEUU, as was discovered in our early efforts in this area (data not shown). However, as a result of its urethane group, PMBU has previously been shown to have an affinity with polyurethanes, and was found to blend well with the PEUU of this study [24]. Both polymers had good solubility in HFIP and the various polymer blends were easily electrospun using a single stream approach. No obvious differences in morphology were observed between PEUU and PEUU/PMBU fibers, even after PBS immersion. Scaffold mechanical properties also showed no significant decreases with the presence of PMBU addition, with the exception of a decrease with 15% PMBU addition. The mechanical properties were still deemed high enough in this case for the target application and the conduits showed compliances in the physiologic range.

As described above, thrombosis and intimal hyperplasia (support of SMC migration and proliferation) are major concerns

for small diameter blood vessel tissue engineering. However, in the setting of a biodegradable vascular graft scaffold the question arises as to how one balances anti-platelet and anti-cell adhesion activity against the need for tissue ingrowth and neo-vessel generation. The amount of PMBU added was shown here to be closely related to the level of inhibition for platelet deposition and smooth muscle cell adhesion and growth. A PMBU content of 15% was chosen for in vivo testing since we considered acute thrombotic risk and early stage intimal hyperplasia to be bigger concerns than ultimate tissue replacement of the scaffold. Our 8 week data would support this position since the PMBU was associated with reduced graft occlusion due to these mechanisms, while evidence of the early stages of tissue replacement was present. Clearly though a longer term study would be needed to evaluate the regeneration question. One might also argue that perhaps an even higher PMBU content might be justified.

Another question arises as to the fate of the added PMBU as the PEUU component of the scaffold is degraded. The ethylene backbone of PMBU would be considered relatively non-degradable, while the urethane bond in the side group of PMBU might be broken gradually by hydrolytic and enzymatic action. By NMR analysis, the urethane bond of PMBU was found to disappear after a 2 week immersion period in an enzyme (lipase) solution (data not shown). If such a cleavage event was to occur in vivo, it should act to diminish the affinity between PMBU and PEUU, and potentially accelerate PMBU elution from the scaffold. Further evaluation of PMBU fate would need to be performed in longer term in vivo experiments. A follow up study in a larger animal model would be appropriate not only to allow for longer evaluation periods, but also for examination of vascular conduits with larger inner diameters and to assess the possibility of late term aneurysmal dilation. The clinical failure of synthetic vascular grafts is inversely related to graft internal diameter and a 1.3 mm inner diameter is arguably an extreme environment. Achieving a routinely patent 3 or 4 mm internal diameter graft would have broad application for coronary and distal extremity bypass procedures. These diameters cannot be effectively evaluated in the current rat model.

6. Conclusions

An elastic, fibrous small diameter vascular scaffold that exhibited good patency and cellularization potential was successfully developed. Blending the MPC copolymer PMBU with PEUU resulted in reduced thrombogenicity and better patency in vivo, while still allowing complete endothelialization and good anastomotic integration. The mechanical properties inherent to the PEUU component, which approximated physiologic compliance values, were maintained with PMBU addition.

Acknowledgements

The authors would like to thank Professor Kazuhiko Ishihara (University of Tokyo, Japan) who kindly provided the PMBU copolymer. This work was financially supported by the NIH grant #HL069368. We also appreciate the expertise of Jennifer Debarr and Nickolas Amoroso for histological staining and Dr. Lara J. Gamble (NESAC/BIO at the University of Washington) for ESCA testing.

Appendix

Figures with essential colour discrimination. Certain figures in this article, in particular parts of Figures 7–10, are difficult to interpret in black and white. The full colour images can be found in the on-line version, at doi:10.1016/j.biomaterials.2009.01.013.

References

- [1] Nerem RM, Seliktar D. Vascular tissue engineering. *Annu Rev Biomed Eng* 2001;3:225–43.
- [2] Couet F, Rajan N, Mantovani D. Macromolecular biomaterials for scaffold-based vascular tissue engineering. *Macromol Biosci* 2007;7:701–18.
- [3] Yow KH, Ingram J, Korossis SA, Ingham E, Homer-Vanniasinkam S. Tissue engineering of vascular conduits. *Br J Surg* 2006;93:652–61.
- [4] Gao J, Crapo P, Nerem R, Wang YD. Co-expression of elastin and collagen leads to highly compliant engineered blood vessels. *J Biomed Mater Res A* 2008;85:1120–8.
- [5] Yang J, Motlagh D, Webb AR, Ameer GA. Novel biphasic elastomeric scaffold for small-diameter blood vessel tissue engineering. *Tissue Eng* 2005;11:1876–86.
- [6] Nieponice A, Soletti L, Guan J, Deasy BM, Huard J, Wagner WR, et al. Development of a tissue-engineered vascular graft combining a biodegradable scaffold, muscle-derived stem cells and a rotational vacuum seeding technique. *Biomaterials* 2008;29:825–33.
- [7] Doi K, Nakayama Y, Matsuda T. Novel compliant and tissue-permeable microporous polyurethane vascular prosthesis fabricated using an excimer laser ablation technique. *J Biomed Mater Res* 1996;31:27–33.
- [8] Lee SJ, Liu J, Oh SH, Soker S, Atala A, Yoo JJ. Development of a composite vascular scaffolding system that withstands physiological vascular conditions. *Biomaterials* 2008;29:2891–8.
- [9] Luong-van E, Grondahl L, Chua KN, Leong KW, Nurcombe V, Cool SM. Controlled release of heparin from poly(epsilon-caprolactone) electrospun fibers. *Biomaterials* 2006;27:2042–50.
- [10] Khorasani MT, Shorqashti S. Fabrication of microporous polyurethane by spray phase inversion method as small diameter vascular grafts material. *J Biomed Mater Res A* 2006;77:253–60.
- [11] Walpoth BH, Roqlenko R, Tikhvinskaia E, Goqolewski S, Schaffner T, Hess OM, et al. Improvement of patency rate in heparin-coated small synthetic vascular grafts. *Circulation* 1998;98: II319–II323, 324.
- [12] Morimoto N, Iwasaki Y, Nakabayashi N, Ishihara K. Physical properties and blood compatibility of surface-modified segmented polyurethane by semi-interpenetrating polymer networks with a phospholipid polymer. *Biomaterials* 2002;23:4881–7.
- [13] Heyligers JMM, Arts CHP, Verhagen HJM, Groot PhG, de Moll FL. Improving small-diameter vascular grafts: from the application of an endothelial cell lining to the construction of a tissue-engineered blood vessel. *Ann Vasc Surg* 2005;19:1–9.
- [14] He W, Ma ZW, Teo WE, Dong YX, Robless PA, Lim TC, et al. Tubular nanofiber scaffolds for tissue engineered small-diameter vascular grafts. *J Biomed Mater Res A* 2008. doi:10.1002/jbm.a.32081. Published online.
- [15] Tillman BW, Yazdani SK, Lee SJ, Geary RL, Atala A, Yoo JJ. The in vivo stability of electrospun polycaprolactone-collagen scaffolds in vascular reconstruction. *Biomaterials* 2009;30:583–8.
- [16] Taite LJ, Yang P, Jun HW, West JL. Nitric oxide-releasing polyurethane-PEG copolymer containing the YIGSR peptide promotes endothelialization with decreased platelet adhesion. *J Biomed Mater Res B Appl Biomater* 2008;84:108–16.
- [17] Shirota T, He H, Yasui H, Matsuda T. Human endothelial progenitor cell-seeded hybrid graft: proliferative and antithrombotic potentials in vitro and fabrication processing. *Tissue Eng* 2003;9:127–36.
- [18] Hashi CK, Zhu YQ, Yang GY, Young WL, Hsiao BS, Wang K, et al. Antithrombotic property of bone marrow mesenchymal stem cells in nanofibrous vascular grafts. *Proc Natl Acad Sci U S A* 2007;104:11915–20.
- [19] Iwasaki Y, Nakabayashi N, Ishihara K. In vitro and ex vivo blood compatibility study of 2-methacryloyloxyethyl phosphorylcholine (MPC) copolymer-coated hemodialysis hollow fibers. *J Artif Organs* 2003;6:260–6.
- [20] Morimoto N, Watanabe A, Iwasaki Y, Akiyoshi K, Ishihara K. Nano-scale surface modification of a segmented polyurethane with a phospholipid polymer. *Biomaterials* 2004;25:5353–61.
- [21] Hasegawa T, Iwasaki Y, Ishihara K. Preparation of blood-compatible hollow fibers from a polymer alloy composed of polysulfone and 2-methacryloyloxyethyl phosphorylcholine polymer. *J Biomed Mater Res* 2002;63:333–41.
- [22] Ishihara K, Hujita H, Yoneyama T, Iwasaki Y. Antithrombotic polymer alloy composed of 2-methacryloyloxyethyl phosphorylcholine polymer and segmented polyurethane. *J Biomater Sci Polym Ed* 2000;11:1183–95.
- [23] Guan J, Sacks MS, Beckman EJ, Wagner WR. Synthesis, characterization, and cytocompatibility of elastomeric, biodegradable poly(ester-urethane)ureas based on poly(caprolactone) and putrescine. *J Biomed Mater Res* 2002;61:493–503.
- [24] Ishihara K, Hanyuda H, Nakabayashi N. Synthesis of phospholipid polymers having a urethane bond in the side chain as coating material on segmented polyurethane and their platelet adhesion-resistant properties. *Biomaterials* 1995;16:873–9.
- [25] Hasegawa T, Iwasaki Y, Ishihara K. Preparation and performance of protein-adsorption-resistant asymmetric porous membrane composed of polysulfone/phospholipid polymer blend. *Biomaterials* 2001;22:243–51.
- [26] Severyn DA, Muluk SC, Vorp DA. The influence of hemodynamics and wall biomechanics on the thrombogenicity of vein segments perfused in vitro. *J Surg Res* 2004;121:31–7.
- [27] Tamada Y, Kulik EA, Ikada Y. Simple method for platelet counting. *Biomaterials* 1995;16:259–61.

- [28] Martin ND, Schaner PJ, Tulenko TN, Shapiro IM, Dimatteo CA, Williams TK, et al. In vivo behavior of decellularized vein allograft. *J Surg Res* 2005;129:17–23.
- [29] Wang XN, Chen CZ, Yang M, Gu YJ. Implantation of decellularized small-caliber vascular xenografts with and without surface heparin treatment. *Artif Organs* 2007;31:99–104.
- [30] Cho SW, Lim JE, Chu HS, Hyun HJ, Choi CY, Hwang KC, et al. Enhancement of in vivo endothelialization of tissue-engineered vascular grafts by granulocyte colony-stimulating factor. *J Biomed Mater Res A* 2006;76:252–63.
- [31] Walles T, Puschmann C, Haverich A, Mertsching H. Acellular scaffold implantation—no alternative to tissue engineering. *Int J Artif Organs* 2003;26:225–34.
- [32] Kim WS, Seo JW, Rho JR, Kim WG. Histopathologic changes of acellularized xenogenic carotid vascular grafts implanted in a pig-to-goat model. *Int J Artif Organs* 2007;30:44–52.
- [33] Bailey SR, Polan JL, Munoz OC, Agrawal MC, Goswami NJ. Proliferation and beta-tubulin for human aortic endothelial cells within gas-plasma scaffolds. *Cardiovasc Radiat Med* 2004;5:119–24.
- [34] Nottelet B, Pektok E, Mandrachi D, Tille JC, Walpoth B, Gurny R, et al. Factorial design optimization and in vivo feasibility of poly(ϵ -caprolactone)-micro and nanofiber-based small diameter vascular grafts. *J Biomed Mater Res A* 2008. doi:10.1002/jbm.a.32023. Published online.
- [35] Hu X, Shen H, Yang F, Bei J, Wang S. Preparation and cell affinity of microtubular orientation-structured PLGA(70/30) blood vessel scaffold. *Biomaterials* 2008;29:3128–36.
- [36] Smith MJ, McClure MJ, Sell SA, Barnes CP, Walpoth BH, Simpson DG, et al. Suture-reinforced electrospun polydioxanone–elastin small diameter tubes for use in vascular tissue engineering: a feasibility study. *Acta Biomater* 2008;4:58–66.
- [37] Cheng ST, Chen ZF, Chen GQ. The expression of cross-linked elastin by rabbit blood vessel smooth muscle cells cultured in polyhydroxyalkanoate scaffolds. *Biomaterials* 2008;29:4187–94.
- [38] Williamson MR, Woollard KJ, Griffiths HR, Coombes AG. Gravity spun polycaprolactone fibers for applications in vascular tissue engineering: proliferation and function of human vascular endothelial cells. *Tissue Eng* 2006;12:45–51.
- [39] Jeong SI, Kim SH, Kim YH, Jung Y, Kwon JH, Kim BS, et al. Manufacture of elastic biodegradable PLCL scaffolds for mechano-active vascular tissue engineering. *J Biomater Sci Polym Ed* 2004;15:645–60.
- [40] Roh JD, Nelson GN, Brennan MP, Mirensky TL, Yi T, Hazlett TF, et al. Small-diameter biodegradable scaffolds for functional vascular tissue engineering in the mouse model. *Biomaterials* 2008;29:1454–63.
- [41] Williamson MR, Black R, Kielty C. PCL–PU composite vascular scaffold production for vascular tissue engineering: attachment, proliferation and bioactivity of human vascular endothelial cells. *Biomaterials* 2006;27:3608–16.
- [42] Uchida T, Ikeda S, Oura H, Tada M, Nakano T, Fukuda T, et al. Development of biodegradable scaffolds based on patient-specific arterial configuration. *J Biotechnol* 2008;133:213–8.
- [43] Stitzel J, Liu J, Lee SJ, Komura M, Berry J, Soker S, et al. Controlled fabrication of a biological vascular substitute. *Biomaterials* 2006;27:1088–94.
- [44] Guan J, Fujimoto KL, Sacks MS, Wagner WR. Preparation and characterization of highly porous, biodegradable polyurethane scaffolds for soft tissue applications. *Biomaterials* 2005;26:3961–71.
- [45] Stankus JJ, Guan J, Wagner WR. Fabrication of biodegradable elastomeric scaffolds with sub-micron morphologies. *J Biomed Mater Res A* 2004;70:603–14.
- [46] Fujimoto KL, Guan J, Oshima H, Sakai T, Wagner WR. In vivo evaluation of a porous, elastic, biodegradable patch for reconstructive cardiac procedures. *Ann Thorac Surg* 2007;83:648–54.
- [47] Stankus JJ, Freytes DO, Badylak SF, Wagner WR. Hybrid nanofibrous scaffolds from electrospinning of a synthetic biodegradable elastomer and urinary bladder matrix. *J Biomater Sci Polym Ed* 2008;19:635–52.
- [48] Guan J, Fujimoto KL, Wagner WR. Elastase-sensitive elastomeric scaffolds with variable anisotropy for soft tissue engineering. *Pharm Res* 2008;25:2400–12.
- [49] Stankus JJ, Soletti L, Fujimoto K, Hong Y, Vorp DA, Wagner WR. Fabrication of cell microintegrated blood vessel constructs through electrohydrodynamic atomization. *Biomaterials* 2007;28:2738–46.
- [50] L'Heureux N, Dusserre N, Konig G, Victor B, Keire P, Wight TN, et al. Human tissue-engineered blood vessels for adult arterial revascularization. *Nat Med* 2006;12:361–5.
- [51] Nakabayashi N, Williams DF. Preparation of non-thrombogenic materials using 2-methacryloyloxyethyl phosphorycholine. *Biomaterials* 2003;24:2431–5.
- [52] Ishihara K, Nomura H, Mihara T, Kurita K, Iwasaki Y, Nakabayashi N. Why do phospholipid polymers reduce protein adsorption? *J Biomed Mater Res* 1998;39:323–30.
- [53] Nakaya T, Li YJ. Phospholipid polymers. *Prog Polym Sci* 1999;24:143–81.
- [54] Iwasaki Y, Sawada S, Ishihara K, Khang G, Lee HB. Reduction of surface-induced inflammatory reaction on PLGA/MPC polymer blend. *Biomaterials* 2002;23:3897–903.
- [55] Salvage JP, Rose SF, Phillips GJ, Hanlon GW, Lloyd AW, Ma IY, et al. Novel biocompatible phosphorylcholine-based self-assembled nanoparticles for drug delivery. *J Control Release* 2005;104:259–70.
- [56] Yoneyama T, Sugihara K, Ishihara K, Iwasaki Y, Nakabayashi N. The vascular prosthesis without pseudointima prepared by antithrombogenic phospholipid polymer. *Biomaterials* 2002;23:1455–9.